Loss-of-function and residual channel activity of connexin26 mutations associated with non-syndromic deafness

R. Bruzzone[a,b,*], V. Veronesi[c], D. Gomès[a], M. Bicego[c], N. Duval[a], S. Marlin[a], C. Petit[a], P. D'Andrea[c], T.W. White[d]

[a] *Departement of Neuroscience, Institut Pasteur, 75015 Paris, France*
[b] *Departement of Clinical Neurobiology, Interdisciplinary Center for Neurosciences (IZN), Im Neuenheimer Feld 364, 69120 Heidelberg, Germany*
[c] *Dipartimento di Biochimica, Biofisica e Chimica delle Macromolecole, University of Trieste, 34127 Trieste, Italy*
[d] *Department of Physiology and Biophysics, SUNY at Stony Brook, Stony Brook, NY 11794-8661, USA*

Received 19 August 2002; revised 25 November 2002; accepted 25 November 2002

First published online 4 December 2002

Edited by Maurice Montal

Abstract **Connexins are the protein subunits of gap junction channels that allow a direct signaling pathway between networks of cells. The specific role of connexin channels in the homeostasis of different organs has been validated by the association of mutations in several human connexins with a variety of genetic diseases. Several connexins are present in the mammalian cochlea and at least four of them have been proposed as genes causing sensorineural hearing loss. We have started our functional analysis by selecting nine mutations in Cx26 that are associated with non-syndromic recessive deafness (DFNB1). We have observed that both human Cx26 wild-type (HCx26wt) and the F83L polymorphism, found in unaffected controls, generated electrical conductance between paired *Xenopus* oocytes, which was several orders of magnitude greater than that measured in water-injected controls. In contrast, most recessive Cx26 mutations (identified in DFNB1 patients) resulted in a simple loss of channel activity. In addition, the V37I mutation, originally identified as a polymorphism in heterozygous unaffected individuals, was devoid of function and thus may be pathologically significant. Unexpectedly, we have found that the recessive mutation V84L retained functional activity in both paired *Xenopus* oocytes and transfected HeLa cells. Furthermore, both the magnitude of macroscopic junctional conductance and its voltage-gating properties were indistinguishable from those of HCx26wt. The identification of functional differences of disease causing mutations may lead to define which permeation or gating properties of Cx26 are necessary for normal auditory function in humans and will be instrumental in identifying the molecular steps leading to DFNB1.**

Key words: Channel; Gap junction; Cochlea; Genetic disease; *Xenopus*

1. Introduction

Gap junctions regulate the passage of inorganic ions and small metabolites between adjoining cells of most animal tissues, thus coupling cells both electrically and metabolically. This type of intercellular communication permits coordinated cellular activity, a critical feature for organ homeostasis during development and adult life of multicellular organisms [1,2]. Intercellular channels are formed by connexins, members of a multigene family that comprises over 20 members in humans. Connexins oligomerize to form single-membrane channels, called connexons, which align in the extracellular space between two cells to complete the intercellular channel. Each connexon comprises six connexins arranged radially around a central pore [3,4] and can contain either a single type of connexin (homomeric), or multiple connexins (heteromeric). Because an intercellular channel spans two plasma membranes, adjacent cells can contribute different types of connexons, giving rise to either homotypic, heterotypic, or heteromeric intercellular channels.

The specific role of connexin channels in the homeostasis of different organs has been validated by the association of mutations in several human connexins with a variety of genetic diseases [5,6]. In particular, morphological and electrophysiological studies have described the presence of gap junctions in the inner ear [7–13], where several connexin genes are expressed, and four connexins are involved in different forms of genetic deafness [14]. Thus, mutations in human Cx26 (HCx26), HCx30, HCx31 and HCx43 (*GJB2*, *GJB6*, *GJB3* and *GJA1* genes) have been linked to both syndromic and non-syndromic forms of hearing loss [15–20].

The genetic evidence linking HCx26 mutations to different forms of deafness has led to re-evaluate the role of gap junction channels in the inner ear, where they have been implicated in many aspects of auditory transmission, including sound response in supporting cells, metabolite exchange between supporting cells, and funneling of potassium back to the endolymph [12,21,22]. It is commonly held that simple loss-of-function mutations in HCx26 can cause one type of non-syndromic recessive deafness, DFNB1, as the most frequent recessive HCx26 mutation is a single base deletion (35delG) that results in a frameshift at position 12 in the coding sequence and premature termination of the protein at amino acid 13 [15,17]. Although more than 50 missense mutations have been reported in DFNB1, the functional consequences have been examined only for few of these [23–25]. As for dominant forms of hearing loss, the involvement of HCx26 mutations has now been firmly established for the dominant form of non-syndromic deafness DFNA3 [26], and in syndromic deafness associated with palmoplantar keratoderma [27]. These mutations encode full-length products containing non-conservative amino acid substitutions and a

*Corresponding author. Fax: (49)-6221-561 397.
E-mail address: bruzzone@urz.uni-hd.de (R. Bruzzone).

0014-5793/02/$22.00
PII: S0014-5793(02)03755-9

dominant negative effect on the channel function of wild-type HCx26 (HCx26wt) has been described [23,27–29].

To gain insight into the molecular and cellular defects associated with HCx26 mutations, we have selected 9 DFNB1 mutations scattered throughout the connexin sequence and have tested their ability to form channels in different expression systems. We have found that, although most mutations resulted in a complete loss of function, the V84L variant exhibited junctional currents that were virtually indistinguishable, in both magnitude and voltage-gating properties, from those determined for HCx26wt. These data suggest that, although V84L retains the ability to form functional channels, other properties (such as unitary conductance, size selectivity, open time probability) may be affected, thus resulting in a functional deficit.

2. Materials and methods

2.1. Molecular cloning

For functional expression studies in *Xenopus* oocytes, HCx26wt was subcloned into the *Bgl*II site of the pSP64T expression vector [30], as previously described [27]. We have analyzed the following mutations distributed throughout the connexin molecule: V37I, W77R, F83L, V84L, L90P, S113R, delE120, M163V, R184P, 235delC. All mutations, designated according to the recommendations of the nomenclature working group [31], were generated by oligonucleotide directed site mutagenesis [32]. For functional expression studies in HeLa cells, HCx26wt and the specified DFNB1 mutations were subcloned into the pIRES-EGFP vector (Clontech, Palo Alto, CA, USA), which permits both the gene of interest and the enhanced form of the *Aequorea victoria* green fluorescent protein (referred to hereafter as GFP) to be translated from a single bicistronic mRNA, allowing an efficient selection of transfected cells. The sequence of all clones was verified using the Dye terminator kit (Perkin-Elmer, Wellesley, MA, USA), as recommended by the manufacturer.

2.2. In vitro transcription, oocyte microinjection and pairing

All constructs subcloned in the SP64T vector were linearized with *Xba*I (New England Biolabs) and capped RNAs were produced using the mMessage mMachine kit (Ambion, Austin, TX). The purity and yield of transcribed RNAs were determined by measuring absorbance at 260/280 nm. Stage V–VI oocytes were collected from adult *Xenopus laevis* females and defolliculated following previously described protocols [33,34]. Cells were cultured in modified Barth's (MB) medium and kept at 18°C for the entire duration of the experiment. For physiological analysis, cells were injected with a total volume of 40 nl of either an antisense oligonucleotide (3 ng/cell), to suppress the endogenous *Xenopus* Cx38, or a mixture of antisense (as above) plus the specified Cx26 RNA (40–120 ng/cell), using a Picospritzer II pressure injector (General Valve, Fairfield, NJ, USA). Following an overnight incubation at 18°C, microinjected oocytes were immersed for a few minutes in hypertonic solution to strip the vitelline envelope, transferred to Petri dishes containing MB medium and manually paired with the vegetal poles apposed.

2.3. In vitro translation and metabolic labeling of connexin proteins

Aliquots (300 ng) of in vitro synthesized RNAs were translated (90 min at 30°C) in a rabbit reticulocyte lysate system (Promega Corporation, Madison, WI, USA), in the presence of [^{35}S]methionine (ICN Pharmaceuticals, Costa Mesa, CA, USA); metabolic labeling of oocytes for biochemical analysis was carried out by incubating cells in the presence of [^{35}S]methionine as previously described in detail [34]. Samples from the in vitro translation and cell lysates were separated on a 13% sodium dodecyl sulfate (SDS) gel and analyzed by fluorography using Hyperfilm (Amersham Biosciences, Buckinghamshire, UK).

2.4. Electrical recordings from oocytes

The functional properties of cell-to-cell channels were assessed by a dual voltage clamp procedure that enabled direct quantitation of junctional conductance [35]. The equipment and software used to program stimulus and data collection paradigms have been described elsewhere [28,34]. Current outputs were filtered at 50 Hz and the sampling interval was 10 ms. For simple measurements of junctional conductance (G_j), both cells of a pair were initially clamped at −40 mV to ensure zero transjunctional potential (V_j) and alternating pulses of ±10–40 mV were imposed on one cell. Current delivered to the cell clamped at −40 mV during the voltage pulse was equal in magnitude to the junctional current, and was divided by the voltage to yield the conductance. To determine the voltage-gating properties of HCx26, transjunctional potentials of opposite polarity were generated by hyperpolarizing or depolarizing one cell in 20 mV steps (over a range of ±100–120 mV), while clamping the second cell at −40 mV. Currents were measured at the end of the voltage pulse, at which time they approached steady state (I_{jss}), and the macroscopic conductance (G_{jss}) was calculated by dividing I_{jss} by V_j. G_{jss} was then normalized to the values determined at ±20 mV and plotted against V_j. Data describing the relationship of G_{jss} as a function of V_j were analyzed using Origin 6.0 (Microcal Software, Northampton, MA, USA) and fit to a Boltzmann relation of the form: $G_{jss} = \{(G_{jmax} - G_{jmin})/(1+\exp[A(V_j - V_0)]\} + G_{jmin}$, where G_{jss} is the steady-state junctional conductance, G_{jmax} (normalized to unity) is the maximum conductance, G_{jmin} is the residual conductance at large values of V_j, and V_0 is the transjunctional voltage at which $G_{jss} = (G_{jmax} - G_{jmin})/2$ [35]. The constant A ($= nq/kT$) represents the voltage sensitivity in terms of gating charge as the equivalent number (n) of electron charges (q) moving through the membrane, k is the Boltzmann constant, and T is the absolute temperature. An alternative gating model that integrates the contribution of the voltage gates of the two connexons, eliminating the need for data splicing between positive and negative V_j ranges, has been recently developed [36]. Although this modified equation provides a more accurate description of the gating behavior of channels that are very sensitive to V_j (e.g. Cx37 and Cx45), in the case of homotypic channels that are fully open at $V_j = 0$ mV, such as those formed by Cx26, it can be postulated that each connexin contributes to half of the voltage-gating characteristics. This assumption allows the splice of the gating profile into two segments that are separately fitted to a single Boltzmann equation, without affecting the accuracy of the voltage-gating analysis [36]. The time constants (τ) of voltage-dependent transitions of junctional conductance were determined using data-fitting functions in Origin 6.0.

2.5. Cell culture and transfection

A clone of HeLa cells essentially devoid of connexins, as assessed by intercellular dye transfer [37], was kindly provided by Prof. Klaus Willeke (University of Bonn, Germany) and cultured according to standard procedures. Control experiments in dual whole-cell patch-clamp configuration confirmed that this clone, in contrast to other HeLa clones, lacked endogenous gap junction channels (Prof. Fabio Mammano, personal communication). Twenty-four hours after plating, cells were transfected with the expression vectors described above using the lipofectamine transfection protocol (Gibco, Invitrogen Corp., Leek, The Netherlands). Experiments were performed 24 h after transfection.

2.6. Protein immunoblot analysis

Proteins were solubilized from cells grown to confluence. Prior to electrophoresis, protein concentration was measured by the bicinchoninic acid method (Pierce, Rockford, IL, USA) with bovine serum albumin as the standard. For each sample, 20 μg of total proteins were separated on 13% SDS gel and then transferred to nitrocellulose. Coomassie Blue staining of identical gels run in parallel confirmed the equal loading of the samples. Western blot analysis was performed as described [38]. Connexin immunoreactivity was probed using a polyclonal antibody anti-rat Cx26 (Zymed) at a 1:1500 dilution.

2.7. Immunofluorescence

Cells grown onto glass coverslips were fixed with 2% paraformaldehyde and processed for fluorescence microscopy as previously described [38]. Connexin immunoreactivity was probed using a 1:250 dilution of a polyclonal anti-rat Cx26 (Zymed) antibody, which was revealed by a tetramethylrhodamine isothiocyanate-conjugated, affinity-purified goat anti-rabbit IgG (Jackson ImmunoResearch Laboratories, West Grove, PA, USA). Coverslips were mounted onto glass slides and visualized under a Leica DMLS fluorescence microscope (Leica Microsystems, Wetzlar, Germany).

2.8. Intercellular dye transfer

Glass capillaries were prepared with a dual-step puller (Narishige) and filled with either a 5% solution of Lucifer Yellow (LY) or with a 0.1% solution of 4′,6′-diamidino-2-phenylindole (DAPI) dihydrochloride, both dissolved in 0.33 M lithium chloride. Individual cells in GFP-expressing clusters were pressure-injected with a pneumatic PLI-100 pico-injector (Medical Systems Corp., Greenvale, NY, USA) mounted onto a Zeiss inverted Axiovert 100 TV microscope (Carl Zeiss, Jena, Germany). For both GFP and LY the filter set was Zeiss 09 (BP450-490/LP520). For DAPI dihydrochloride the filter set was Zeiss 21 (BP340-380/LP500). Intercellular LY diffusion was revealed by capturing three different images for each experiment. Image 1, showing GFP-expressing cells before injection; image 2, containing the fluorescence of both GFP and LY; and image 3, resulting from the subtraction of image 1 from image 2, thus displaying LY fluorescence alone [25,28].

2.9. Statistical analysis

Results are shown as the mean ± S.E.M. Comparisons between two populations of data were made with the unpaired Student's *t*-test; *P* values less than 0.05 were considered to be significant.

3. Results

3.1. Biochemical characterization of DFNB1 mutations

We have used the paired oocyte expression system to assess the functional consequences of Cx26 mutations associated with DFNB1. In this assay, two oocytes are manipulated together to form a pair from which intercellular currents developed by the injected connexin RNAs can be quantified and analyzed. For all the constructs, the translational competence of the in vitro transcribed RNAs was examined in a rabbit reticulocyte lysate in the presence of [^{35}S]methionine (Fig. 1A). The radioactive products were separated by SDS-gel electrophoresis and detected by fluorography. Translation reactions that contained RNAs encoding any of the HCx26 mutations (lanes 3–13) produced a predominant band of the same apparent size as that of HCx26wt (lane 2). The deletion of one amino acids at residue 120 (lane 10) did not change appreciably the migration of the protein product under the experimental conditions used. As expected, the 80 amino acid polypeptide, which resulted from the translation of the truncated 235delC RNA, could not be separated from the migration front under these experimental conditions (lane 13). A translation reaction receiving only water synthesized no major protein products (lane 1). We then verified that *Xenopus* oocytes were also able to support the synthesis of the wild-type and mutated constructs (Fig. 1B). Metabolically labeled oocytes injected with water produced a characteristic pattern of [^{35}S]-labeled proteins (lane 1). Injection of RNA for either HCx26wt, or any of the DFNB1 mutations tested (except for the truncated 235delC), resulted in the appearance of a novel band, which migrated as HCx26wt and was easily identified over the pattern of labeled endogenous proteins (Fig. 1B). The W44C mutation, associated with the dominant form of deafness DFNA3, is shown here for comparison (lane 4). Together, these experiments demonstrate that oocytes can support the biosynthesis of all HCx26 constructs. Although HCx26wt was not synthesized very efficiently, in comparison to other connexins [33,34], all mutations were expressed at the same or higher levels, suggesting that any functional differences with HCx26wt could not be simply ascribed to defective protein biosynthesis and/or stability.

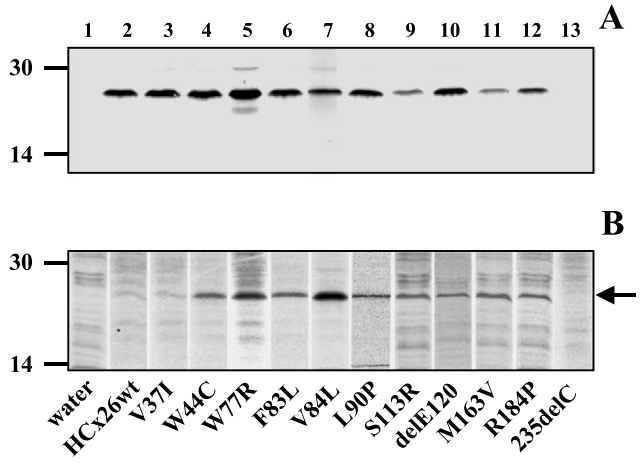

Fig. 1. Translational competence of synthetic RNAs encoding HCx26wt and the mutations analyzed. Experimental conditions are indicated on top of each lane. The molecular mass (in kDa) and migration of protein standards are indicated on the left edge of each gel. A: In vitro translated RNA induced the synthesis of a major polypeptide product migrating with the expected electrophoretic mobility, except for the truncated 235delC, which resulted in a protein of approximately 9 kDa that could not be separated from the migration front. B: Metabolic labeling of *Xenopus* oocytes showed that HCx26wt and all mutations directed the appearance of a specific band with an electrophoretic mobility similar to that of the in vitro synthesized products.

Table 1
Junctional conductance developed by homotypic *Xenopus* oocyte pairs expressing wild-type human Cx26 (HCx26wt) and mutations linked to non-syndromic deafness

RNA injection	Junctional conductance (μS)	Number of pairs
Water	0.023 ± 0.006	25
HCx26wt	3.646 ± 0.817	24
V37I	0.013 ± 0.003	15
W77R	0.013 ± 0.005	24
F83L	2.623 ± 0.862	15
V84L	4.012 ± 0.864	16
L90P	0.014 ± 0.003	18
S113R	0.013 ± 0.004	13
delE120	0.028 ± 0.009	13
M163V	0.018 ± 0.004	21
R184P	0.020 ± 0.006	10
235delC	0.013 ± 0.004	13

Oocytes were co-injected with the specified cRNAs and an oligonucleotide antisense to mRNA for *Xenopus* Cx38 to eliminate the possible contribution of endogenous coupling to the recorded conductances. Water-injected cells were used as negative controls. Cells were then stripped of the vitelline envelope in hypertonic medium and paired with the vegetal poles facing each other 24–48 h prior to electrophysiological measurements. Values are mean ± S.E.M. of the number of pairs indicated. All conditions were tested in at least three separate batches of oocytes.

3.2. Functional expression of DFNB1 mutations in paired *Xenopus* oocytes

The ability of DFNB1 mutations to form homotypic intercellular channels (that is with both connexons composed of the same connexin) was tested using the paired *Xenopus* oocyte expression system (Table 1). Although Cx26 is not known to interact with the endogenous *Xenopus* Cx38, all experiments were performed with oocytes pretreated with antisense oligonucleotides to ensure that the observed currents were the result of the exogenously supplied connexins. As previously reported [34,39], water-injected cells showed no detectable

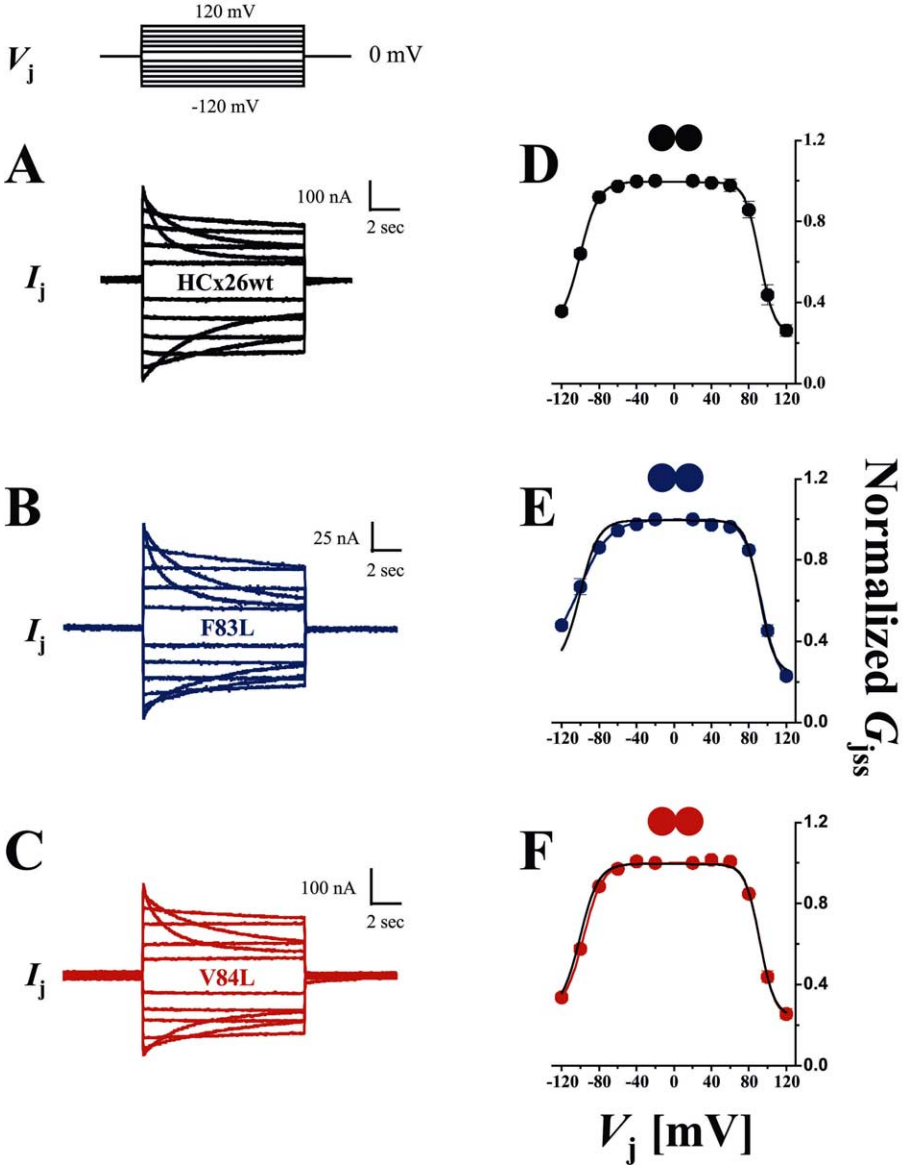

Fig. 2. Voltage-gating properties of intercellular channels formed by V84L are similar to those of HCx26wt. A–C: Families of currents illustrating the time-dependent decay of junctional currents (I_j) induced by transjunctional voltage (V_j) steps of increasing amplitude and opposite polarity (top traces). At $V_j \geq 80$ mV, consistent decreases in I_j were observed for HCx26wt (A), or the F83L polymorphism (B), or the DFNB1-associated V84L mutation (C). D–F: Plots describe the relationship of V_j to steady-state junctional conductance (G_{jss}) normalized to the values measured at ± 20 mV. All channels exhibited a similarly high threshold of voltage dependence. Smooth lines represent the best fits to the Boltzmann equation of the form indicated in Section 2, for which the parameters are given in Table 2. The Boltzmann fits of HCx26wt are also shown in panels E and F for comparison (black lines). Results are the mean ± S.E.M. of five to six pairs whose G_j values at the beginning of the experiment are given in Table 2.

coupling under these conditions, indicating that a virtually complete suppression of endogenous currents had been achieved (Table 1). Injection of RNAs for eight (V37I, W77R, L90P, S113R, delE120, M163V, R184P, 235delC) out of the 10 mutations analyzed did not induce the formation of homotypic junctional channels, since the levels of conductance measured never exceeded background values (Table 1). In contrast, the V84L mutation efficiently assembled homotypic channels and induced conductance levels of the same order of magnitude as those developed by homotypic pairs expressing either HCx26wt or the F83L polymorphism (Table 1 and Fig. 2). Thus, one DFNB1 mutation is functionally competent to form intercellular channels in paired oocytes.

3.3. *Voltage-gating properties of V84L channels are similar to HCx26wt*

Although V84L retained the ability to form functional channels, it remained possible that some of its electrical properties and gating behavior were altered. To address this issue, we compared the response of homotypic V84L channels to voltage gating. Typical transjunctional currents and plots of the relationship between steady-state junctional conductance (G_j) and transjunctional voltage (V_j) are presented in Fig. 2. Voltage steps lasted 10 s to allow currents to approach equilibrium values. The junctional currents of HCx26wt pairs decayed slowly over time for potentials greater than 60 mV (Fig. 2A), in agreement with previous studies that utilized the ro-

Table 2
Comparison of Boltzmann parameters of intercellular channels composed of wild-type (wt) and mutant HCx26 expressed in paired *Xenopus* oocytes

Channel	V_j	G_{jmax}	G_{jmin}	A	n	V_0
HCx26wt/HCx26wt	+	1	0.24	0.13	3.2	92
F83L/F83L	+	1	0.18	0.11	2.6	94
V84L/V84L	+	1	0.23	0.12	3.1	92
HCx26wt/HCx26wt	−	1	0.27	0.10	2.5	100
F83L/F83L	−	1	0.31	0.06	1.5	102
V84L/V84L	−	1	0.27	0.10	2.5	96

Oocytes were co-injected with the specified cRNAs and an oligonucleotide antisense to mRNA for *Xenopus* Cx38, stripped of the vitelline envelope and paired for 24–48 h prior to electrophysiological measurements. Junctional conductance (G_j) developed between pairs of *Xenopus* oocytes was measured by dual voltage clamp in response to increasing transjunctional potentials (V_j) of opposite polarity and normalized to the conductance measured at a V_j of ±20 mV (G_{jmax}, set as unity), as described in Section 2. Data were fit to a Boltzmann equation of the form given in the text. G_{jmin} is the minimum conductance value as estimated from the Boltzmann fit, and V_0 is the voltage at which half-maximal decrease of G_j is measured. The cooperativity constant (A), reflecting the voltage sensitivity of the channel, can also be expressed as the equivalent number (n) of electron charges moving through the transjunctional field. The plus and minus signs for V_j refer to the polarity of the transjunctional potential. These parameters were derived from oocyte pairs whose G_j (mean ± S.E.M.) was 3.2 ± 0.7 μS (n = 5) for HCx26wt/HCx26wt; 2.0 ± 0.6 μS (n = 6) for F83L/F83L; and 2.1 ± 0.6 μS (n = 6) for V84L/V84L.

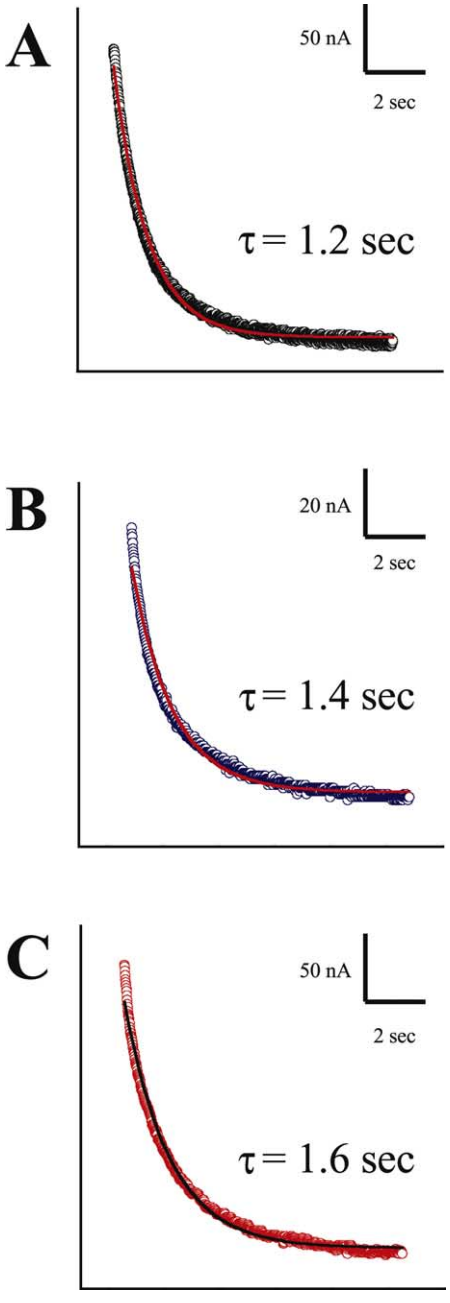

dent homologs [39]. It was also noted that the junctional current decay was slightly asymmetrical, i.e. the rate of decline over the duration of the voltage step tended to be greater for positive values of V_j. Conductance values measured at the end of the imposed pulses were normalized to those recorded at the lower transjunctional potential (i.e. ±20 mV) and plotted against the increasing V_j of either polarity. Fitting the data from five pairs to the Boltzmann equation of the form given in Section 2 (Fig. 2D, smooth lines) revealed that the transjunctional voltage (V_0) required to elicit a conductance midway between G_{jmax} and G_{jmin} had a value of 92 mV for positive V_js, and a value of −100 mV for negative V_js. Among mammalian connexins, only Cx36 exhibits such a low threshold of V_j gating, with a V_0 around ±100 mV [40–42]. The same characteristics were also observed when we analyzed intercellular channels made of either the F83L polymorphism (Fig. 2B,E), or the V84L mutation associated with DFNB1 (Fig. 2C,F), as indicated by virtual superposition of their Boltzmann fits to those calculated for HCx26wt.

To analyze the kinetics of voltage gating, the current decay at a V_j of +100 mV was fit to a first-order exponential function plus a constant term. For HCx26wt (Fig. 3A), the rate of channel closure yielded time constants of 1.2 s. The present values are somewhat distinct from the kinetic data recorded from oocytes expressing rodent Cx26, which exhibited a slower transition (5–6 s) from high to low conductance at a V_j of +100 mV [39]. Junctional currents of F83L (Fig. 3B) and V84L (Fig. 3C) were also best fit by a first-order exponential decay functions with time constants of 1.4 and 1.6 s, respectively The similarities in the τ values between HCx26wt, F83L and V84L were also evident for negative V_js, although currents decayed with slower time constants (not shown). Taken together, these data indicate that the voltage-gating properties of the V84L mutations do not significantly differ from those of HCx26wt.

←
Fig. 3. Kinetic analysis of voltage-dependent channel closure. Current decays after the imposition of a +100 mV transjunctional voltage (V_j) step could be well fit by a monoexponential relation with the time constants (τ) indicated. Time-dependent closure of mutant V84L channels was similar to that of HCx26wt and the F83L polymorphism.

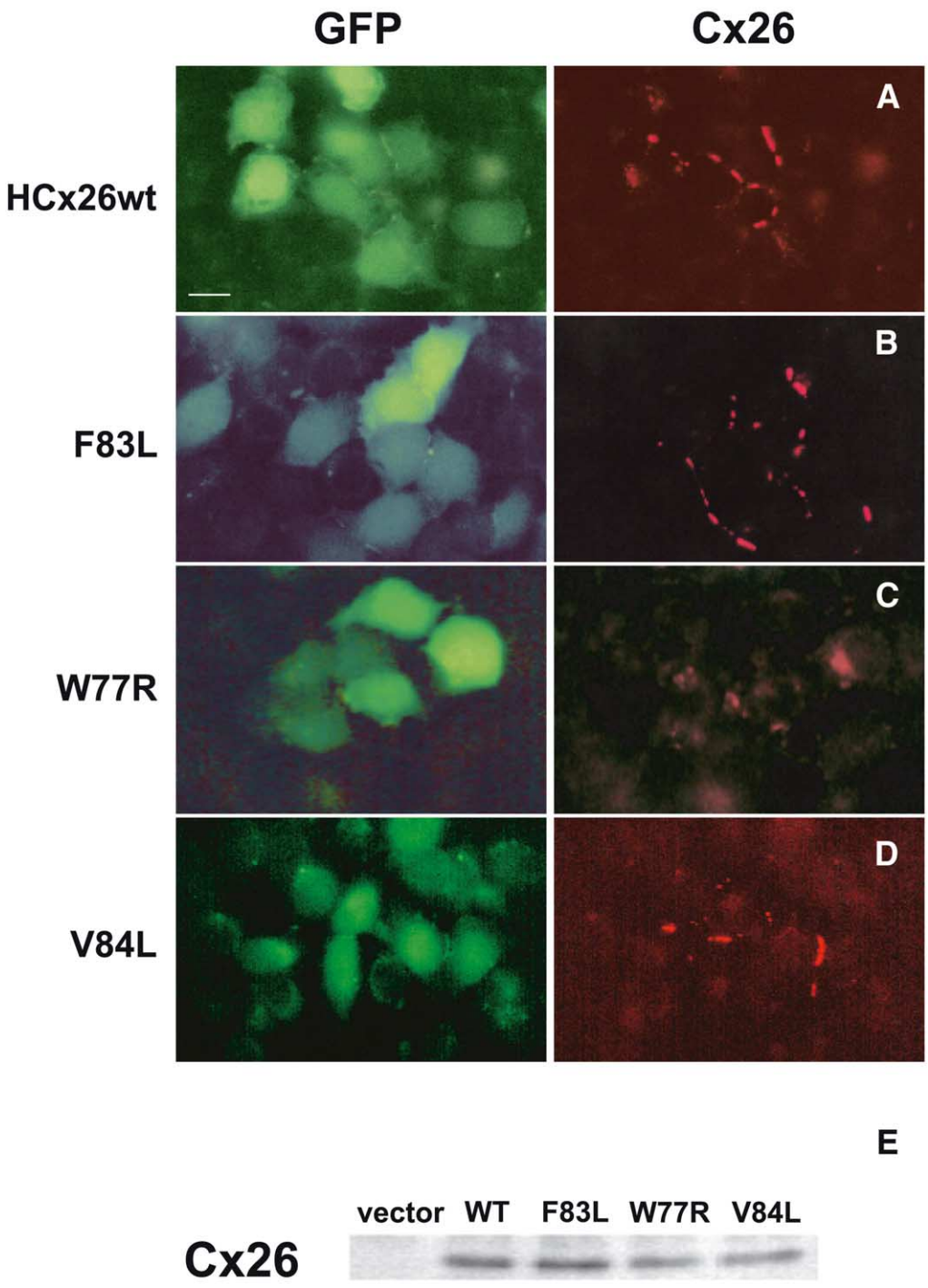

Fig. 4. Expression of HCx26wt and deafness-associated mutations in HeLa cells. Expression of GFP in transfected HeLa cells resulted in a diffuse cytoplamsic staining (left-hand-side panels). Immunolocalization of Cx26 in GFP-expressing cells showed a characteristic punctate staining in the case of HCx26wt (A), the F83L polymorphism (B) and the V84L mutation (D), whereas W77R (C) exhibited a predominantly cytoplasmic labeling pattern (right-hand-side panels). Scale bar is 10 μm for all panels. E: Western blot analysis of protein expression demonstrated that comparable levels of protein expression were obtained.

3.4. V84L channels are permeable to fluorescent tracers

It has been previously reported that two mutations of HCx32 associated with the X-linked form of Charcot–Marie–Tooth (CMTX) disease, S26L and M34T, produce functional channels with reduced permeability to molecules that can permeate HCx32wt channels [43]. Thus, we have used HeLa cells to investigate whether the permeability of the V84L mutation to fluorescent tracers was altered. All constructs were transiently transfected in HeLa cells using an expression vector that allows both the gene of interest and the enhanced form of *A. victoria* GFP to be translated from a single bicistronic mRNA. Transfection with HCx26wt and the F83L polymorphism produced, in GFP-positive cells, a dashed, membrane-associated staining typical of gap junctional plaques, indicat-

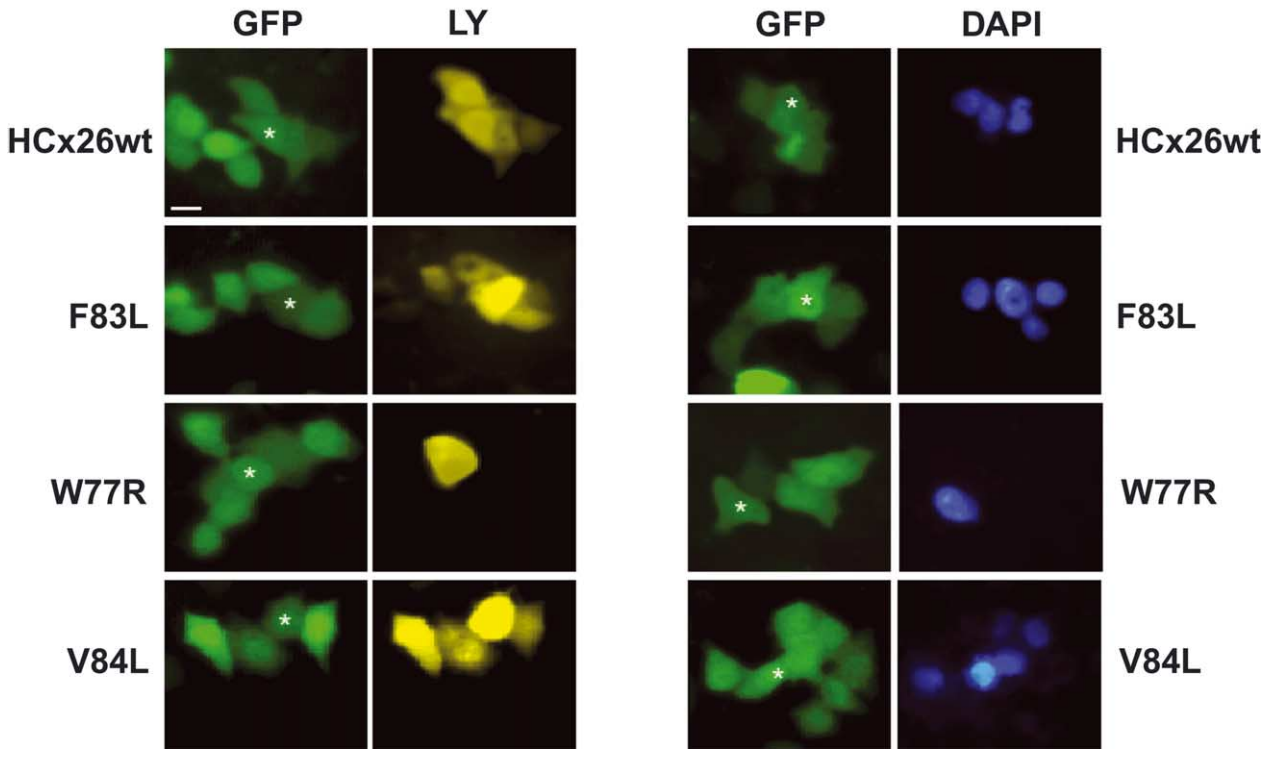

Fig. 5. Functional investigation of deafness-associated HCx26 mutations by dye coupling. Individual cells in clusters expressing GFP were microinjected with either LY or DAPI, and the intercellular diffusion of the dye was monitored 5 min after the injection. For each construct, clusters of GFP-expressing cells before injection are shown in the left-hand-side panels, whereas the corresponding LY and DAPI fluorescence are presented in the right-hand-side panels. Intercellular coupling was present between cells expressing HCx26wt, the F83L polymorphism and the V84L mutation, whereas W77R-transfected cells were uncoupled. Asterisks denote the injected cells. Scale bar is 10 μm for all panels.

ing that they were correctly targeted to the plasma membrane (Fig. 4A,B). As expected, in cells transfected with vector alone, no Cx26 staining could be detected (not shown). The immunolocalization of the V84L mutation gave results similar to HCx26wt, with junctional plaques at the areas of cell-to-cell apposition (Fig. 4D). In contrast, another DFNB1 mutation used for comparison, W77R, gave a predominantly cytoplasmic labeling pattern (Fig. 4C). To examine to which extent Cx26 mutations affected the level of protein expression, Western blot experiments were performed on total lysates of transiently transfected cells ($n = 3$ from three independent transfections). For all constructs, proteins of the predicted molecular mass and comparable levels of expression were observed (Fig. 4E).

We next analyzed the permeability of the same constructs to the intercellular transfer of LY in clusters of cells transiently expressing either HCx26wt or the mutated connexins (Fig. 5, cf. GFP and LY). Non-transfected HeLa cells, used as a negative control, did not display intercellular dye transfer (not shown), confirming that the clone was devoid of basal intercellular coupling [37]. Microinjection of LY in cells expressing either HCx26wt ($n = 51$) or the F83L ($n = 27$) polymorphism induced intercellular coupling in 100% of the cases, with 100% of GFP-positive cells being filled with the fluorescent tracer, whereas no dye transfer was observed between clusters of cells expressing W77R ($n = 31$). Interestingly, V84L ($n = 45$) showed the same high incidence and extent of dye transfer as HCx26wt. Similar results were obtained by microinjecting HeLa cells with DAPI dihydrochloride (Fig. 5, cf. GFP and DAPI), with 100% of transfer being recorded in cells transfected with HCx26wt ($n = 32$), F83L ($n = 16$) and V84L ($n = 21$) whereas no instance of dye coupling was observed with W77R ($n = 10$). Together, these experiments indicate that, in HeLa cells, the V84L mutation is correctly targeted to areas of cell–cell apposition where it forms functional channels that are permeable to fluorescent tracers.

4. Discussion

Genetic deafness is one of the most prevalent inherited sensory disorders, affecting about 1 in 2000 children in developed countries. Despite the fact that more than 20 loci have been described for non-syndromic autosomal recessive deafness, a high proportion of all cases is due to HCx26, the gene mutated in the DFNB1 form [14]. Currently, over 50 missense mutations scattered along the HCx26 protein have been described [44] and individuals carrying them present a variable audiological phenotype that could be dependent on either a different functional role of each mutated allele, its possible residual activity or the influence of environmental and genetic factors. In this study, we have analyzed the functional consequences of nine DFNB1 mutations of HCx26 by testing their ability to form intercellular channels in the paired *Xenopus* oocytes expression system. Our results demonstrate that, although the majority of mutations resulted in a complete loss of function, one retained the ability to form functional gap junction channels (Fig. 6). These findings extend the observations that a group of CMTX mutations of HCx32 also exhibit residual functional activity [43,45–47].

Previous studies had mainly examined the functional prop-

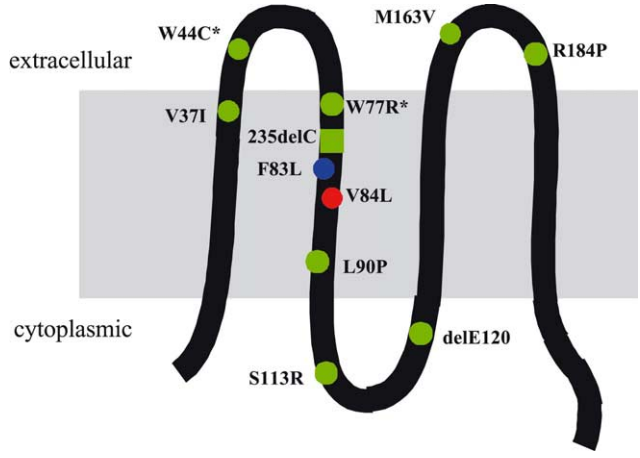

Fig. 6. Schematic topology relative to the plasma membrane of HCx26. The approximate position of the mutations associated with non-syndromic deafness that have been analyzed is shown. They were all missense mutations, except for delE120, which originated from a single codon deletion, and for 235delC, which is a single base deletion that introduces a stop codon at position 80 (square). The F83L polymorphism is shown in blue. Mutations that result in a loss of function are shown in green, whereas the DFNB1-linked V84L variant, which retains functional activity, is shown in red. *W44C was analyzed in refs. [28,29]; W77R was also studied in refs. [23,24,27].

erties of dominant HCx26 mutations associated with either syndromic or non-syndromic hearing loss [23,27–29,48]. The present study extends these observations by demonstrating that a number of DFNB1 mutations scattered along the HCx26 protein have all lost the ability to form intercellular channels. The cellular basis of this functional loss remains to be established. As previously reported for CMTX mutations of HCx32 [49,50], the mutated protein may interfere with either one of several steps, including stability of the protein, assembly into connexons, targeting to the plasma membrane, alignment and docking between the two connexons to form the complete intercellular channel. The biochemical analysis of HCx26 expression in oocytes shows that all mutations were synthesized at least as efficiently as HCx26wt. Thus, their failure to induce intercellular channels could not be the result of much reduced protein levels. In addition, a functional screening of HCx26 mutations provides a useful means to test the pathogenicity of heterozygous mutations detected in unaffected controls. Thus, we have obtained functional evidence that the F83L sequence variant [51] is a non-pathological polymorphism. In contrast, we have found that the valine to isoleucine substitution at position 37 (V37I), which had been previously described as a polymorphism in a US population where it did not segregate with deafness [52], is devoid of functional activity. These data rather suggest that V37I causes hearing loss and corroborate a more recent mutational analysis [53] that identified two individuals with sensorineural deafness, one of whom is homozygous for this mutation, whereas the other is a compound heterozygote with the commonest pathological mutation, 35delG.

The unexpected finding of this study is that one DFNB1 mutation is capable of forming intercellular channels as efficiently as HCx26wt. The valine to leucine at amino acid 84 (V84L) mutation has been reported in two individuals who were compound heterozygotes for the 35delG mutation [52], where a guanine (G) in a sequence of six G is deleted, resulting in a premature stop codon at position 13. Furthermore, two unaffected individuals in the same pedigree carried the V84L mutation and a normal allele. Because the prevalence of 35delG in several European countries has been estimated at 2–4% of the normal hearing population [54,55] it was concluded that the V84L mutation in the second allele was responsible for the hearing loss documented in these two patients. Although the pathological significance of this mutation may be difficult to explain, a valine to alanine substitution at this residue has been recently reported in patients with non-syndromic hearing loss in the Korean population [56].

The analysis of some of the functional properties of V84L channels indicate that their voltage-gating behavior and permeability to tracers are remarkably similar to those of HCx26wt channels. Thus, conductance decreased only at relatively high transjunctional potentials and the transjunctional voltage (V_0) required to elicit a conductance midway between G_{jmax} and G_{jmin} had a value of 92 mV for positive V_js, for both HCx26wt and V84L. Furthermore, the kinetic properties of channel closure seen for V84L closely matched those of HCx26wt and the F83L polymorphism. In all cases, the decay of the junctional current was best fit by a first-order exponential function with comparable time constants. To test whether V84L exhibited a different permeability to tracer molecules, we used two fluorescent probes that differ in size, charge and other physical constants: LY (MW = 443, with two negative charges) and DAPI (MW = 279, with one positive charge). Our experiments indicate that HeLa cells expressing V84L transfer LY and DAPI to about the same extent as HCx26wt and the F83L polymorphism, suggesting no major change in channel permeability. It remains possible that a systematic approach, using the dual whole-cell patch-clamp technique to introduce molecules of different radius in the cytoplasm of one cell, may be needed to detect a more subtle alteration of channel permeability. For example, it has been calculated that molecules with a radius of 3.1 Å are excluded from intercellular channels made of a functional CMTX mutation of HCx32, whereas the pore radius of wild-type HCx32 is approximately twice the size of the mutated channel, between 6 and 7 Å [43].

Together with the genetic evidence that at least four connexins underlie different forms of deafness, our results suggest that the complement of connexins in the inner ear serves specific functions and the loss or the functional alteration of a single connexin species is detrimental. Gap junctions in the organ of Corti have been proposed to be implicated in several processes of auditory transmission, including the funneling of potassium ions from the perilymph to the *stria vascularis* where the endocochlear potential is generated and synchronization of cellular responses in the region of maximal mechanical stimulation [12,14,21,22,57,58]. It is difficult to reconcile this model with the available data on potassium permeation through gap junction channels, as all connexin channels are readily permeable to this cation [59] and the loss of a single cochlear connexin would still leave other functional connexins available to perform this task. For example, Cx26 and Cx30 participate in the formation of two independent cellular networks [11,12,60]: one is composed of fibrocytes and mesenchymal cells, whereas the other connects the supporting cells of the inner hair cells and outer hair cells, and the adjacent epithelial cells. Although gap junctions have been historically described as relatively non-selective, permeable to a wide va-

riety of molecules with a size smaller than ~1200 Da [61], connexin channels do show differential permeability to a wide range of other small molecules and second messengers [37,59,62–64]. Thus, an alternative possibility is that the V84L mutation may interfere with the ability to assemble heteromeric and/or heterotypic channels with other connexins expressed in the inner ear, thereby changing not only the macroscopic levels of communication, but also significantly altering the range of molecules being exchanged between the coupled cells. This hypothesis is in agreement with electrophysiological data that are indicative of heterotypic and/or heteromeric connexin channels between cochlear supporting cells [65], and with recent observations obtained in mice with a conditional inactivation of Cx26 in the inner ear epithelium [66]. The characterization of these animals, which exhibit hearing impairment, suggests that lack of Cx26 does not affect vestibular and cochlear development, but may play an essential role in the survival of the supporting sensory epithelium at the onset of hearing. In this context, it is plausible that the network of Cx26 channels accounts for the spatial buffering of K+ and/or glutamate that are released by inner sensory cells upon sound stimulation, thereby preventing toxic effects that result from their extracellular accumulation [66].

Acknowledgements: We thank Marie-Madeleine Gabellec for skillful technical assistance, Klaus Willecke (University of Bonn, Germany) for the generous gift of the communication-incompetent HeLa clone, and Fabio Mammano (Venetian Institute of Molecular Medicine, Padua, Italy) for sharing with us the results of dual whole-cell patch-clamp experiments with the same HeLa clone. This work was supported by grants from the Association Française Contre les Myopathies and RETINA France (to R.B.), the European Community and the Association Française contre les Myopathies (to C.P.), the University of Trieste, Telethon grant GP0043Y02 and the Regione Friuli Venezia-Giulia (to P.D'A.), and NIH grants EY13163, AR47102, and DC05491 (to T.W.W.). During part of this work, P.D'A. was the recipient of a short-term fellowship from the Human Frontier Science Program.

References

[1] Bruzzone, R., White, T.W. and Paul, D.L. (1996) Eur. J. Biochem. 238, 1–27.
[2] Willecke, K., Eiberger, J., Degen, J., Eckardt, D., Romualdi, A., Güldenagel, M., Deutsch, U. and Söhl, G. (2002) Biol. Chem. 383, 725–737.
[3] Yeager, M. and Nicholson, B.J. (1996) Curr. Opin. Struct. Biol. 6, 183–192.
[4] Unger, V.M., Kumar, N.M., Gilula, N.B. and Yeager, M. (1999) Science 283, 1176–1180.
[5] White, T.W. and Paul, D.L. (1999) Annu. Rev. Physiol. 61, 283–310.
[6] Bennett, M.V.L. and Abrams, C.K. (2000) in: Gap Junctions (Peracchia, C., Ed.), pp. 423–459, Academic Press, San Diego, CA.
[7] Dunn, R.A. and Morest, D.K. (1975) Proc. Natl. Acad. Sci. USA 72, 3599–3603.
[8] Iurato, S., Franke, K., Luciano, L., Wermber, G., Pannese, E. and Reale, E. (1976) Acta Otolaryngol. 82, 57–69.
[9] Nadol Jr., J.B., Mulroy, M.J., Goodenough, D.A. and Weiss, T.F. (1976) Am. J. Anat. 147, 281–301.
[10] Santos-Sacchi, J. and Dallos, P. (1983) Hear. Res. 9, 317–326.
[11] Kikuchi, T., Adams, L.C., Paul, D.L. and Kimura, R.S. (1994) Acta Otolaryngol. 114, 520–528.
[12] Kikuchi, T., Kimura, R.S., Paul, D.L. and Adams, J.C. (1995) Anat. Embryol. 191, 101–118.
[13] Mammano, F., Goodfellow, S.J. and Fountain, E. (1996) NeuroReport 7, 537–542.
[14] Petit, C., Levilliers, J. and Hardelin, J-P. (2001) Annu. Rev. Genet. 35, 589–646.
[15] Denoyelle, F., Weil, D., Maw, M.A., Wilcox, S.A., Lench, N.J., Allen-Powell, D.R., Osborn, A.H., Dahl, H.H., Middleton, A., Houseman, M.J., Dode, C., Marlin, S., Boulila-ElGaied, A., Grati, M., Ayadi, H., BenArab, S., Bitoun, P., Lina-Granade, G., Godet, J., Mustapha, M., Loiselet, J., El-Zir, E., Aubois, A., Joannard, A. and Petit, C. (1997) Hum. Mol. Genet. 6, 2173–2177.
[16] Kelsell, D.P., Dunlop, J., Stevens, H.P., Lench, N.J., Liang, J.N., Parry, G., Mueller, R.F. and Leigh, I.M. (1997) Nature 387, 80–83.
[17] Zelante, L., Gasparini, P., Estivill, X., Melchionda, S., D'Agruma, L., Govea, N., Mila, M., Monica, M.D., Lutfi, J., Shohat, M., Mansfield, E., Delgrosso, K., Rappaport, E., Surrey, S. and Fortina, P. (1997) Hum. Mol. Genet. 6, 1605–1609.
[18] Richard, G., Smith, L.E., Bailey, R.A., Itin, P., Hohl, D., Epstein, E.H.J., DiGiovanna, J.J., Compton, J.G. and Bale, S.J. (1998) Nat. Genet. 20, 366–369.
[19] Xia, J.H., Liu, C.Y., Tang, B.S., Pan, Q., Huang, L., Dai, H.P., Zhang, B.R., Xie, W., Hu, D.X., Zheng, D., Shi, X.L., Wang, D.A., Xia, K., Yu, K.P., Liao, X.D., Feng, Y., Yang, Y.F., Xiao, J.Y., Xie, D.H. and Huang, J.Z. (1998) Nat. Genet. 20, 370–373.
[20] Grifa, A., Wagner, C.A., D'Ambrosio, L., Melchionda, S., Bernardi, F., Lopez-Bigas, N., Rabionet, R., Arbones, M., Monica, M.D., Estivill, X., Zelante, L., Lang, F. and Gasparini, P. (1999) Nat. Genet. 23, 16–18.
[21] Santos-Sacchi, J. (2000) Brain Res. Rev. 32, 167–171.
[22] Lagostena, L., Cicuttin, A., Inda, J., Kachar, B. and Mammano, F. (2001) Cell Commun. Adhes. 8, 393–399.
[23] White, T.W., Deans, M.R., Kelsell, D.P. and Paul, D.L. (1998) Nature 394, 630–631.
[24] Martin, P.E.M., Colbam, S.L., Casalotti, S.O., Forge, A. and Evans, W.H. (1999) Hum. Mol. Gen. 8, 2369–2376.
[25] D'Andrea, P., Veronesi, V., Bicego, M., Melchionda, S., Zelante, L., Di Iorio, E., Bruzzone, R. and Gasparini, P. (2002) Biochem. Biophys. Res. Commun. 296, 685–691.
[26] Denoyelle, F., Lina-Granade, G., Plauchu, P., Bruzzone, R., Chaïb, H., Lévi-Acobas, F., Weil, D. and Petit, C. (1998) Nature 393, 319–320.
[27] Richard, G., White, T.W., Smith, L.E., Bailey, R.A., Compton, J.G., Paul, D.L. and Bale, S.J. (1998) Hum. Genet. 103, 393–399.
[28] Bruzzone, R., Gomès, D., Denoyelle, F., Duval, N., Perea, J., Veronesi, V., Weil, D., Petit, C., Gabellec, M-M., D'Andrea, P. and White, T.W. (2001) Cell Commun. Adhes. 8, 425–431.
[29] Rouan, F., White, T.W., Brown, N., Taylor, A.M., Lucke, T.W., Paul, D.L., Munro, C., Uitto, J., Hodgins, M. and Richard, G. (2001) J. Cell Sci. 114, 2105–2113.
[30] Krieg, P.A. and Melton, D.A. (1984) Nucleic Acids Res. 12, 7057–7070.
[31] Antonarakis, S.E. (1998) Hum. Mutat. 11, 1–3.
[32] Ausubel, F.M., Brent, R., Kingston, R.E., Moore, D.D., Seidman, J.G., Smith, J.A. and Struhl, K. (1992) Short Protocols in Molecular Biology, Wiley, New York.
[33] Swenson, K.I., Jordan, J.R., Beyer, E.C. and Paul, D.L. (1989) Cell 57, 145–155.
[34] Bruzzone, R., Haefliger, J-A., Gimlich, R.L. and Paul, D.L. (1993) Mol. Biol. Cell 4, 7–20.
[35] Spray, D.C., Harris, A.L. and Bennett, M.V.L. (1981) J. Gen. Physiol. 77, 77–93.
[36] Chen-Izu, Y., Moreno, A.P. and Spangler, R.A. (2001) Am. J. Physiol. 281, C1604–C1613.
[37] Elfgang, C., Eckert, R., Lichtenberg-Fraté, H., Butterweck, A., Traub, O., Klein, R.A., Hülser, D.F. and Willecke, K. (1995) J. Cell Biol. 129, 805–817.
[38] Romanello, M. and D'Andrea, P. (2001) J. Bone Miner. Res. 16, 1465–1476.
[39] Barrio, L.C., Suchyna, T., Bargiello, T., Xu, L.X., Roginski, R.S., Bennett, M.V.L. and Nicholson, B.J. (1991) Proc. Natl. Acad. Sci. USA 88, 8410–8414.
[40] Srinivas, M., Rozental, R., Kojima, T., Dermietzel, R., Mehler, M., Condorelli, D.F., Kessler, J.A. and Spray, D.C. (1999) J. Neurosci. 19, 9848–9855.
[41] Al-Ubaidi, M.R., White, T.W., Ripps, H., Poras, I., Avner, P., Gomès, D. and Bruzzone, R. (2000) J. Neurosci. Res. 59, 813–826.
[42] Teubner, B., Degen, J., Söhl, G., Güldenagel, M., Bukauskas,

F.F., Trexler, E.B., Verselis, V.K., De Zeeuw, C.I., Lee, C.G., Kozak, C.A., Petrasch-Parwez, E., Dermietzel, R. and Willecke, K. (2000) J. Membr. Biol. 176, 249–262.
[43] Oh, S., Yi, R., Bennett, M.V.L., Trexler, E.B., Verselis, V.K. and Bargiello, T.A. (1996) Neuron 19, 927–938.
[44] Rabionet, R., Gasparini, P. and Estivill, X. (2002) http://www.iro.es/cx26deaf.html.
[45] Omori, Y., Mesnil, M. and Yamasaki, H. (1996) Mol. Biol. Cell 7, 907–916.
[46] Ressot, C., Gomès, D., Dautigny, A., Pham-Dinh, D. and Bruzzone, R. (1998) J. Neurosci. 18, 4063–4075.
[47] Abrams, C.K., Oh, S., Ri, Y. and Bargiello, T.A. (2000) Brain Res. Rev. 32, 203–214.
[48] White, T.W. (2000) Brain. Res. Rev. 32, 181–183.
[49] Deschênes, S.M., Walcott, J.L., Wexler, T.L., Scherer, S.S. and Fischbeck, K.H. (1997) J. Neurosci. 17, 9077–9084.
[50] VanSlyke, J.K., Deschenes, S.M. and Musil, L.S. (2000) Mol. Biol. Cell 11, 1933–1946.
[51] Scott, D.A., Kraft, M.L., Carmi, R., Ramesh, A., Elbedour, K., Yairi, Y., Srisailapathy, C.R., Rosengren, S.S., Markham, A.F., Mueller, R.F., Lench, N.J., Van Camp, G., Smith, R.J. and Sheffield, V.C. (1998) Hum. Mutat. 11, 387–394.
[52] Kelley, P.M., Harris, D.J., Comer, B.C., Askew, J.W., Fowler, T., Smith, S.D. and Kimberling, W.J. (1998) Am. J. Hum. Genet. 62, 792–799.
[53] Wilcox, S.A., Saunders, K., Osborn, A.H., Arnold, A., Wunderlich, J., Kelly, T., Collins, V., Wilcox, L.J., McKinlay Gardner, R.J., Kamarinos, M., Cone-Wesson, B., Williamson, R. and Dahl, H.H. (2000) Hum. Genet. 106, 399–405.
[54] Estivill, X., Fortina, P., Surrey, S., Rabionet, R., Melchionda, S., D'Agruma, L., Mansfield, E., Rappaport, E., Govea, N., Mila, M., Zelante, L. and Gasparini, P. (1998) Lancet 351, 394–398.
[55] Storm, K., Willocx, S., Flothmann, K. and Van Camp, G. (1999) Hum. Mutat. 14, 263–266.
[56] Park, H.J., Hahn, S.H., Chun, Y.M., Park, K. and Kim, H.N. (2000) Laryngoscope 110, 1535–1538.
[57] Johnstone, B.M., Patuzzi, R., Syka, J. and Sykova, E. (1989) J. Physiol. 408, 77–92.
[58] Oesterle, E.C. and Dallos, P. (1990) J. Neurophysiol. 64, 617–636.
[59] Harris, A.L. (2001) Q. Rev. Biophys. 34, 325–472.
[60] Lautermann, J., ten Cate, W.J.F., Altenhoff, P., Grümmer, R., Traub, O., Frank, H., Jahnke, K. and Winterhager, E. (1998) Cell Tissue Res. 294, 415–420.
[61] Simpson, I., Rose, B. and Loewenstein, W.R. (1977) Science 195, 294–297.
[62] Veenstra, R.D. (1996) J. Bioenerg. Biomembr. 28, 327–337.
[63] Bevans, C.G., Kordel, M., Rhee, S.K. and Harris, A.L. (1998) J. Biol. Chem. 273, 2808–2816.
[64] Cao, F.L., Eckert, R., Elfgang, C., Nitsche, J.M., Snyder, S.A., Hülser, D.F., Willecke, K. and Nicholson, B.J. (1998) J. Cell Sci. 111, 31–43.
[65] Zhao, H.B. and Santos-Sacchi, J. (2001) J. Membr. Biol. 175, 17–24.
[66] Cohen-Salmon, M., Ott, T., Michel, V., Hardelin, J.-P., Perfettini, I., Eybalin, M., Wu, T., Marcus, D.C., Wangemann, P., Willecke, K. and Petit, C. (2002) Curr. Biol. 12, 1106–1111.